



# Optimizing Interface Conductivity in Electronics



The latest eBook from  
**Advanced Optical Metrology.**  
Download for free.

Surface roughness is a key parameter for judging the performance of a given material's surface quality for its electronic application. A powerful tool to measure surface roughness is 3D laser scanning confocal microscopy (LSM), which will allow you to assess roughness and compare production and finishing methods, and improve these methods based on mathematical models.

Focus on creating high-conductivity electronic devices with minimal power loss using laser scanning microscopy is an effective tool to discern a variety of roughness parameters.

**EVIDENT**  
**OLYMPUS**

**WILEY**

# Synthesis and Evaluation of Novel Functional Polymers Derived from Renewable Jasmine Lactone for Stimuli-Responsive Drug Delivery

Kuldeep Kumar Bansal,<sup>\*</sup> Ezgi Özliseli, Ari Rosling, and Jessica Marianne Rosenholm<sup>\*</sup>

Instances of synthetic polymers obtained from renewable feedstock with the possibility of post-synthesis functionalization are scarce. Herein, the first ever synthesis and drug delivery application of amphiphilic block copolymer (mPEG-b-PJL) derived from renewable jasmine lactone with free allyl groups on the backbone is presented. The polymer is synthesized via facile ring-opening polymerization and subsequently, UV mediated thiol-ene click chemistry is utilized for post-functionalization. The introduction of hydroxyl, carboxyl, and amine functionality to mPEG-b-PJL polymer is successfully established. As a proof-of-concept demonstration, doxorubicin (DOX) is conjugated on hydroxyl-terminated polymer (mPEG-b-PJL-OH) via redox responsive disulfide linkage to obtain PJL-DOX. PJL-DOX is readily self-assembled into micelles with an average hydrodynamic size of  $\approx 150$  nm and demonstrates reduction-responsive DOX release. Micelles are evaluated in vitro for cytocompatibility and selective drug release in cancer cells (MDA-MB-231) using 10 mM glutathione as a reducing agent. Cytotoxicity and microscopy results confirm a redox-triggered release of DOX, which is further confirmed by flow cytometry. The introduction of these novel functional polymers can pave the way forward in designing polymer-drug conjugate-based smart nano-carriers.

solutions.<sup>[1]</sup> Polymers and more specifically, polyesters have gained a significant position in drug delivery mainly owed to their well-controlled biodegradability. Poly(lactic acid) (PLA), and its copolymers such as poly(lactic-co-glycolic acid) (PLGA), are the ideal examples of polyesters derived from renewable feedstock that can further be produced via facile ring-opening polymerization (ROP) with full control on polymer structure. Nevertheless, poor drug loading is often observed with PLA-based materials owing to its low hydrophobicity and thus, more hydrophobic versions of PLA have been prepared to increase the stability and hydrophobicity of PLA-based drug delivery carriers.<sup>[2]</sup> However, synthesis of these alkyl-substituted lactides seems tedious and thus, a straightforward methodology of preparing amphiphilic block copolymer using renewable poly(decalactone) (PDL) was recently reported. PDL-based drug delivery carriers were evaluated largely for their toxicity, biodegradability, and their potential as drug delivery carriers.<sup>[3–6]</sup>

## 1. Introduction


Polymers derived from renewable feedstock have gained prominent attention in recent years as a sustainable alternative to fossil-based materials due to the depletion of fossil fuels and government policies, which are aiming to promote greener

Since PDL is an amorphous polymer, PDL-based micelles demonstrate a rapid drug release along with initial burst release. In the absence of control over drug release, premature drug leakage is usually observed from micelles during storage and/or after administration in the human body (before reaching the actual target site), which could lead to suboptimal therapeutic activity.<sup>[7]</sup> In recent years, polymer-drug conjugates (PDCs) have emerged as an effective approach to circumvent the problems associated with premature drug release and to improve the overall efficiency of therapy. In addition, conjugation of polymers to the therapeutics offers improved pharmacokinetic and pharmacodynamic properties such as increased plasma half-life, protection of the drug/bioactives degradation from degrading enzymes, enhanced stability of proteins, and enhanced solubility of low-molecular-weight drugs.<sup>[8]</sup> Moreover, drug conjugation via stimuli-responsive linkers affords additional control over the drug release at selective target sites.<sup>[9]</sup>

The availability of free functional groups on the polymer backbone is a crucial pre-requisite for the development of efficient PDCs. Several reports have been published discussing the approaches for preparing functional polyesters<sup>[10]</sup> but literatures presenting their drug delivery applications are rare, owing to the complex design and limited functionality. For instance,

Dr. K. K. Bansal, E. Özliseli, Prof. J. M. Rosenholm  
Pharmaceutical Sciences Laboratory, Faculty of Science and Engineering  
Åbo Akademi University  
Turku 20520, Finland  
E-mail: kuldeep.bansal@abo.fi; jessica.rosenholm@abo.fi

Dr. K. K. Bansal, Prof. A. Rosling  
Laboratory of Polymer Technology  
Centre of Excellence in Functional Materials at Biological Interfaces  
Åbo Akademi University  
Biskopsgatan 8, Turku 20500, Finland

 The ORCID identification number(s) for the author(s) of this article can be found under <https://doi.org/10.1002/adfm.202101998>.

© 2021 The Authors. Advanced Functional Materials published by Wiley-VCH GmbH. This is an open access article under the terms of the Creative Commons Attribution License, which permits use, distribution and reproduction in any medium, provided the original work is properly cited.

DOI: 10.1002/adfm.202101998



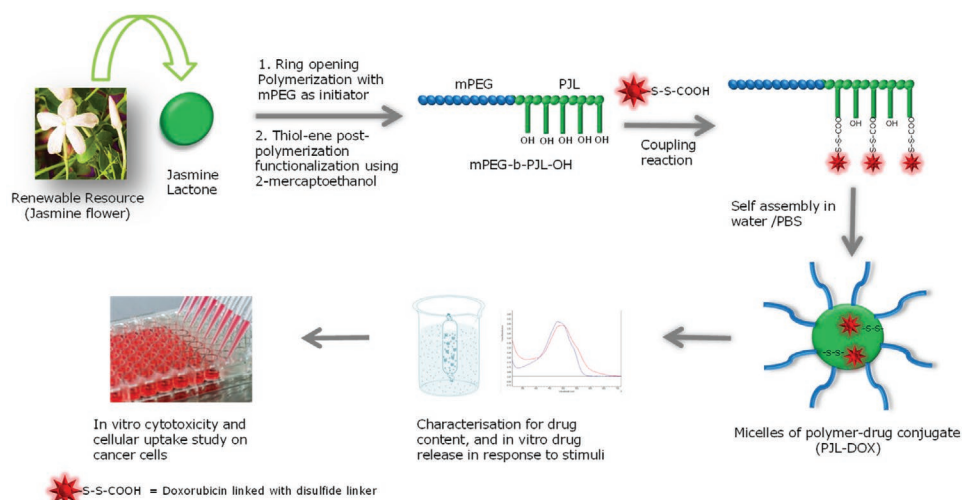


**Figure 1.** Graphical illustration of the preparation and evaluation of novel PjL polymer-based stimuli-responsive drug delivery system.

poly(glutamic acid) (PGA) was utilized for conjugation of camptothecin, and the resultant product (CT-2106) entered clinical trials. However, the polymer PGA is limited to drug molecules that have free alcohol groups for conjugation. Moreover, the reaction conditions require protection and de-protection steps and thus, is not an industrial friendly approach.<sup>[11]</sup> Another successful synthetic polymer used for fabricating PDCs to date is poly(ethylene glycol) (PEG), and approximately twelve such formulations are available on the market.<sup>[8]</sup> However, non-degradability, poor drug loading due to lack of functional groups (type and number), and PEG immunogenicity limit its applications. Consequently, some PEG-based products were withdrawn from the market.<sup>[12]</sup>

A simplistic and reproducible design of biodegradable polymer with the scope of excellent tunability as per desired drug delivery application using economical/renewable feedstock is still the major key point for successful translation of polymer-based drug delivery systems from bench to bedside. Monomers containing free “ene” groups in their backbone are of immense interest for polymer synthesis due to the possibilities it offers to insert functional groups of interest via facile thiol-ene click reaction. Moreover, the “ene” group does not interfere in the ROP reactions, which is one of the most acceptable and reliable reaction mechanisms to produce high molecular-weight polyesters with precise chain length. The ROP of functional renewable monomer  $\alpha$ -methylene- $\gamma$ -butyrolactone (MBL) is one of the best examples, which was utilized to generate polymers with “ene” handles.<sup>[13]</sup> However, specific catalysts and stringent reaction conditions are required to acquire polymers using MBL, which restrict its widespread applications and are apparent from the lack of published reports presenting the applications of poly(MBL).

The polymer science domain is still looking for a polymer, which can be synthesized easily with ample possibilities of post functionalization as per the desired requirement. Therefore, here, we are presenting the synthesis, characterization, and one of the several possible applications of a novel polymer, called poly(jasmine lactone) (PjL) with functional handles. Subsequently, we have designed a PjL-drug conjugate using doxorubicin (DOX) as a drug, with disulfide bond as a reduction

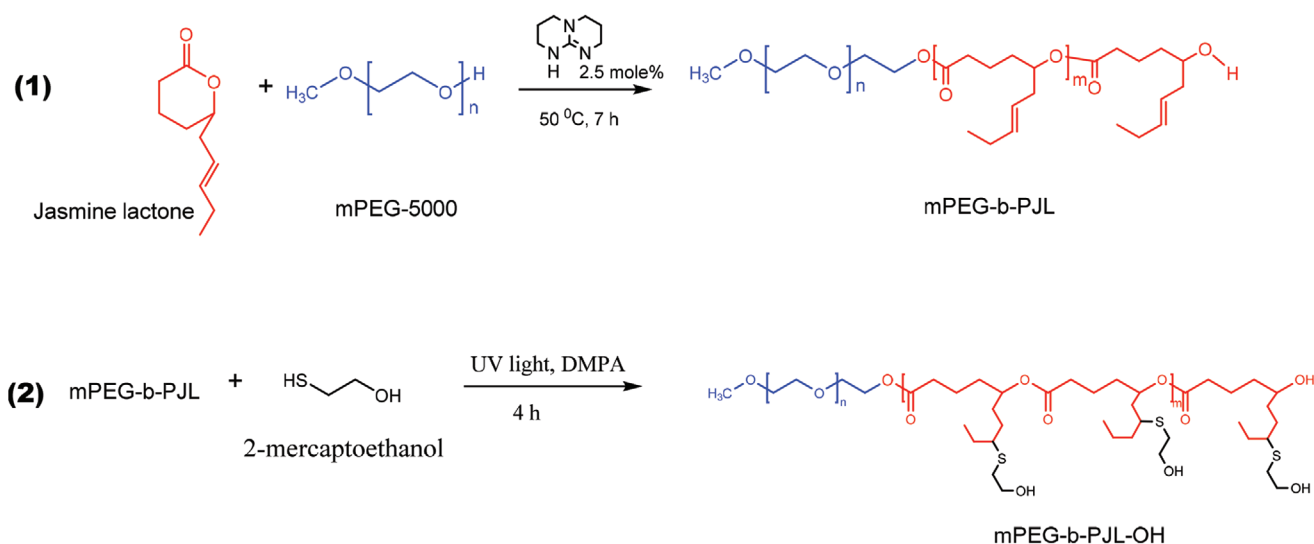
sensitive linker to demonstrate the selective drug release capability in the presence of glutathione (GSH) (**Figure 1**). It is widely reported that disulfide linker cleaved in the presence of GSH, which is usually found in high levels within cancer cells compared to normal cells.<sup>[14,15]</sup> Thus, selective drug release in cancer treatment could be highly beneficial considering the serious side effects of chemotherapy.

The polymer is produced via a facile methodology using renewable monomer (jasmine lactone) with generous modification possibilities. Jasmine lactone is a United States Food and Drug Administration approved food additive and a Generally Recognized As Safe (GRAS) substance, found in several natural substances including jasmine oil, tea, lily, ginger, peach, etc. This monomer provides two unique properties: 1) polymer synthesis in a highly controlled fashion via well-established ROP technique and 2) possibility of post-polymerization functionalization via facile thiol-ene click reaction without additional efforts, such as protection-deprotection. To the best of our knowledge, this is the very first report discussing the synthesis, post-functionalization, and drug delivery capability of PjL.

## 2. Results and Discussion

### 2.1. Synthesis and Characterization of PjL based Polymers

The ROP is quite a robust technique for the synthesis of polymers using lactone monomers in a highly controlled fashion. Metal-free ROP of six-membered rings unfolds the pathway of using renewable monomers for polymer synthesis.<sup>[16]</sup> Thus, inspired by our previous work on  $\delta$ -decalactone, we decided to utilize jasmine lactone for polymer synthesis considering the possibilities of post-functionalization using thiol-ene click reactions. The amphiphilic block copolymer of PjL was prepared at 50 °C using methoxy(polyethylene glycol) (mPEG) as the initiator in the absence of solvents (**Scheme 1**). The purified polymer was characterized by Fourier-transform infrared spectroscopy (FTIR), <sup>1</sup>HNMR, and size exclusion chromatography (SEC) to confirm the structure and molecular weight.



**Scheme 1.** 1) Synthesis scheme of jasmine lactone block copolymer via ring-opening polymerization using mPEG<sub>5k</sub> as initiator and 1,5,7-triazabicyclo[4.4.0]dec-5-ene (TBD) as catalyst. 2) The block copolymer mPEG-b-PJL was later functionalized via UV-light induced thiol-ene click reaction to insert free alcohol groups (mPEG-b-PJL-OH). Since the post-functionalization reaction is not regioselective, thiol is attached randomly to either 2nd or 3rd carbon of the pendant chain of jasmine lactone. Thiol is used in excess for complete conversion of “ene” groups available on mPEG-b-PJL.

The structure of block copolymer of PJL is almost identical to the previously reported PDL-based polymers, except for the availability of an “ene” group on the PJL side chain. The FTIR and <sup>1</sup>HNMR analysis implied successful conversion of monomer to polymer, and observed peaks were matched with the PDL polymer.<sup>[4]</sup> The maximum conversion observed for jasmine lactone using 1,5,7-triazabicyclo[4.4.0]dec-5-ene as catalyst was 88%, and a similar phenomenon was observed for the ROP of  $\delta$ -decalactone, which also never reached 100% due to the polymerization thermodynamics.<sup>[16]</sup> The “ene” group peaks were observed at 5.3 and 5.5 ppm and the percentage conversion, as well as molecular weight, was calculated by comparing the proton peak resonance at 3.3 ppm (methyl group of PEG), 4.2 ppm (newly formed ester bond) and at 4.9 ppm (shifted peak from 4.3 ppm after ring-opening of jasmine lactone) (Figures S1 and S2B, Supporting Information). The proton resonance of “ene” group peaks in <sup>1</sup>HNMR suggested the attachment of  $\approx 24$  repeating units of a monomer onto mPEG.

Next, to establish the multifunctional viability of PJL, we prepared polymers with different free functional groups. The “ene” groups present on the backbone of PJL were converted into hydroxyl, carboxyl, and amine end groups via UV mediated thiol-ene click reaction<sup>[17]</sup> (Scheme 1 and Figure S1, Supporting Information). The details of the synthesized polymers are presented in **Table 1**. Interestingly, no conversion was observed when cysteamine was used as a thiol moiety. A similar phenomenon was reported earlier where cysteamine failed to participate in thiol-ene reaction owing to amine basicity.<sup>[18]</sup> Conversely, close to 100% conversion was observed using Boc protected cysteamine suggesting that the amine basicity has a direct impact on thiol-ene reaction in this case (data not included). However, since our objective is to design simplistic methods for the development of functional polymers, and thus to avoid additional deprotection steps, we utilized cysteamine hydrochloride for generating amine-terminated

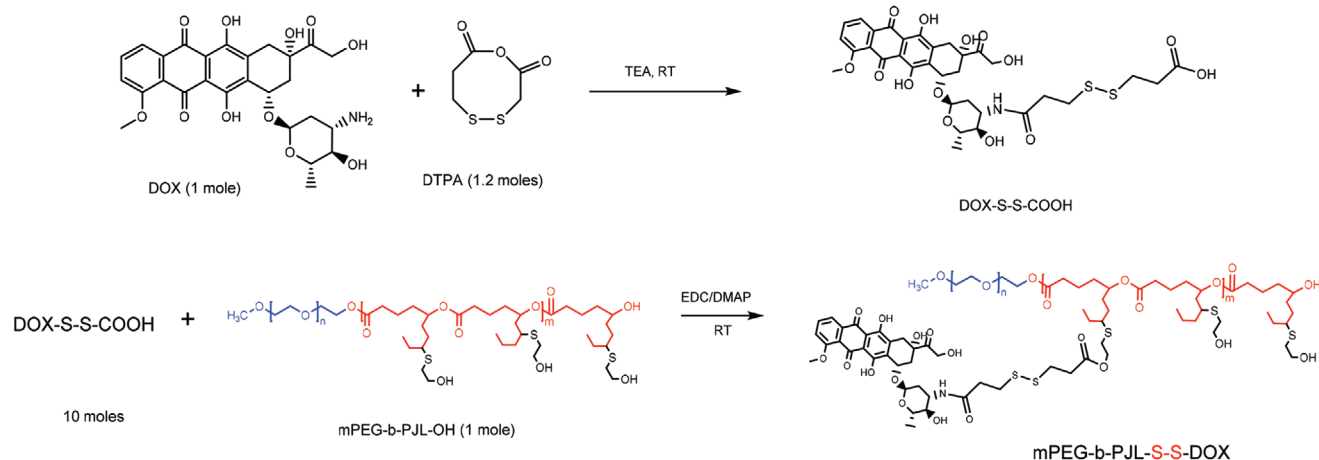
polymer. However, conversion of amine to its hydrochloric salt in cysteamine was not good enough to suppress the amine basicity completely, and thus we only observed a maximum of 70% of conversion.

The disappearance of the “ene” group peaks (730 cm<sup>-1</sup> in FTIR and at 5.3 and 5.5 ppm in <sup>1</sup>HNMR) was monitored to determine the success of thiol-ene reaction (Figures S3 to S5, Supporting Information). Since the substitution of thiol on “ene” of PJL is not regioselective, two peaks for methyl group at  $\approx 1.0$  ppm were observed. 100% substitution of “ene” groups was observed for hydroxyl and carboxyl terminated polymer as evident by <sup>1</sup>HNMR. However, proton peaks at 5.3 and 5.5 ppm corresponding to “ene” groups are observed for amine-terminated polymer due to the incomplete reaction (Figure S5B, Supporting Information). SEC traces using THF as solvent and polystyrene as standard suggested unimodal size distribution of mPEG-b-PJL, mPEG-b-PJL-OH, and mPEG-b-PJL-COOH with a low polydispersity index ( $\mathcal{D}$ ) (Table 1 and Figure S6, Supporting Information). All the obtained characterization data suggested successful synthesis of the block copolymer of PJL as well as post-functionalization to generate –OH, –COOH, and –NH<sub>2</sub> end group polymers.

**Table 1.** Molecular weight of different polymers analyzed by NMR and SEC (ND-not determined).

S.No.	Polymer Name	Mn by <sup>1</sup> HNMR <sup>a)</sup> [kDa]	Mn by SEC [kDa]	$\mathcal{D}$ ( $M_w/M_n$ )
1	mPEG-b-PJL	9.0	8.8	1.4
2	mPEG-b-PJL-OH	10.7	9.4	1.4
3	mPEG-b-PJL-COOH	11.4	9.8	1.4
4	mPEG-b-PJL-NH <sub>2</sub> .HCl	10.8	ND	ND

<sup>a)</sup>Molecular weight was calculated by comparing the proton integral of mPEG at 3.3 ppm and PJL at 4.8 and 5.3 ppm (in case of functional polymers to determine the consumption of “ene” groups).



**Scheme 2.** Schematic representation of the conjugation of DOX to the polymer chain via reduction sensitive di-sulfide linker. DTPA- dithiodipropionic anhydride, TEA- triethylamine, EDC- 1-Ethyl-3-(3-dimethylaminopropyl)carbodiimide, DMAP- dimethylamino pyridine, RT- room temperature.

## 2.2. Preparation and Evaluation of PjL-Drug Conjugate

Polymers with free functional groups are valuable for designing PDCs to achieve high drug loading. Thus, to explore the benefits of functional PjL polymer and to establish the stimuli-responsive drug delivery capability, mPEG-b-PjL-OH was selected for further evaluation. The critical micelle concentration (CMC) of the polymer was evaluated using pyrene fluorescence peak intensity ratio method to ensure mPEG-b-PjL-OH is capable of self-assembly to generate micelles.<sup>[4]</sup> The peak intensity of pyrene is influenced greatly by the polarity shift in the surrounding environment where the peak at 375 nm is dominant in aqueous surroundings while the peak at 393 nm is dominant in hydrophobic surroundings (Figure S7A, Supporting Information). As the micelles start forming, the pyrene in water start migrating to the hydrophobic core of the micelles (most favorable place for hydrophobic compound) and thus the peak ratio starts declining. A curve was plotted between peak intensity ratio and polymer concentration and the inflection point of the curve was selected as the CMC of the polymer, which is found to be  $8.9 \mu\text{g mL}^{-1}$  (Figure S7B, Supporting Information).

DOX was used as a drug candidate in this study considering that despite being a potent drug, its widespread use in chemotherapy is restricted due to severe cardiotoxicity.<sup>[19]</sup> Disulfide linker was selected to conjugate the DOX with mPEG-b-PjL-OH. Disulfide is a well-known linker and has been utilized in several studies to produce stimuli-responsive drug delivery systems that are cleaved in highly reductive environments, which is usually observed in tumor regions.<sup>[9]</sup> Dithiodipropionic acid was used to prepare a disulfide linker and converted into protected anhydride form (i.e., dithiodipropionic anhydride, DTPA) to control its reactivity via a reported procedure.<sup>[15]</sup> The conversion of acid into anhydride was confirmed by FTIR, where a clear peak of C=O anhydride stretching was observed at  $1793 \text{ cm}^{-1}$  (Figure S8, Supporting Information). To make the conjugation process simpler, a one-pot reaction scheme was followed where DOX was first reacted with DTPA, followed by activation of acid end group via 1-Ethyl-3-(3-dimethylaminopropyl)

carbodiimide and coupling of mPEG-b-PjL-OH using dimethylamino pyridine as catalyst (Scheme 2). The reactions were monitored by following the consumption of DOX via thin-layer chromatography.

After reaction completion, the conjugate mPEG-b-PjL-S-S-DOX (PjL-DOX) was purified by dialysis and freeze-dried for further evaluation. The absence of free DOX in conjugate was ascertained by HPLC (Figure S9, Supporting Information), where the disappearance of the peak at retention time 9.1 (DOX peak) in PjL-DOX sample confirms the purification of polymer conjugate. However, the appearances of three peaks in PjL-DOX HPLC trace suggest a random number of DOX molecules conjugation onto the polymer chain. We presumed that the peak at 18.6 min indicates the PjL-DOX with the highest number of DOX molecules (owing to increased hydrophobicity). To determine the number of DOX molecules attached onto mPEG-b-PjL-OH, a <sup>1</sup>HNMR analysis was performed. Out of 10 molecules,  $\approx 9$  DOX molecules were attached to mPEG-b-PjL as calculated by comparing the proton integral for DOX at 7.75 ppm, mPEG at 3.3 ppm, and PjL at 0.98 ppm (Figure S4B, Supporting Information). The weight % drug loading was determined by UV-Vis spectroscopy as no substantial change in  $\lambda_{\text{max}}$  of DOX was observed after its conjugation onto the polymer (Figure S10A, Supporting Information). The DOX content in PjL-DOX was found to be 30% by weight. It should be noted that we have used a 1:10 molar ratio of polymer:DOX for the conjugation reaction despite having 24 available conjugation sites. Thus, we believe that a higher drug loading could be possible when 100% of the available conjugation sites will be utilized. Moreover, we anticipated that the steric hindrance during conjugation reaction would not be the limiting factor due to the amorphous nature (chain flexibility) of PjL.

Remarkably, the freeze-dried powder of PjL-DOX in the absence of any cryoprotectants was found to be easily dispersible in water without the need for additional measures. Generally, it has been reported that the freeze-drying process significantly affects the particle size upon reconstitution and thus, a large amount of cryoprotectant is often required to protect the structure of amphiphilic polymer-based

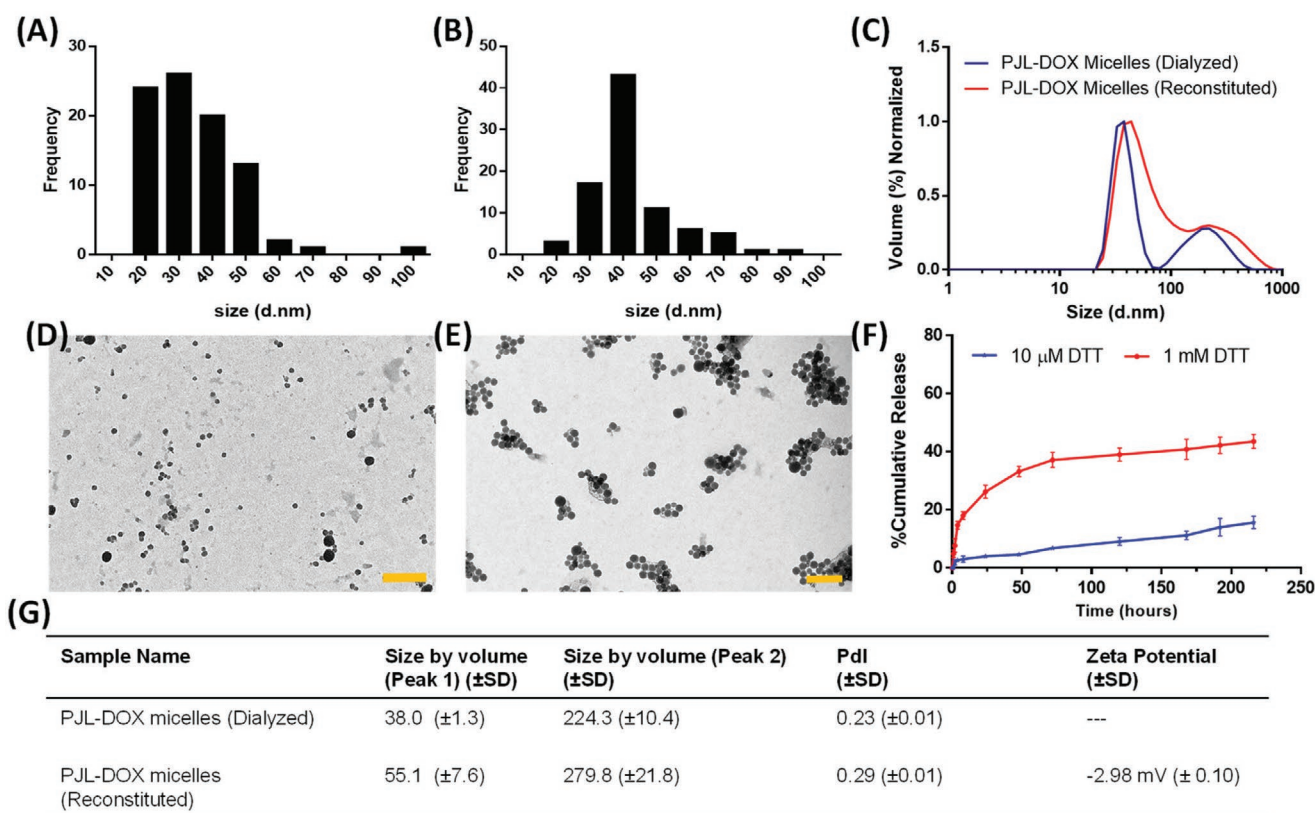


**Figure 2.** Size distribution evaluation of PJJ-DOX micelles as determined by TEM imaging (via ImageJ), A) analyzed directly after dialysis, B) prepared by reconstituting in water, and C) by DLS. TEM micrographs of micelles D) prepared by dialysis and E) reconstituted (scale = 200 nm). F) In vitro release of DOX from reconstituted PJJ-DOX micelles in the presence of different concentrations of DTT at 37 °C in acetate buffer (0.1 M, pH = 5.0), and G) size details (in diameter) estimated by DLS for both micelle types.

nanoparticles/micelles.<sup>[20]</sup> Since the dried products are more stable compared to solutions/suspensions in terms of long-term storage, PJJ polymer-based drug delivery systems might be the better alternative for such solution/suspension-based nanoparticles currently on the market. The easy dispersibility of conjugate (up to the tested concentration of 4 mg mL<sup>-1</sup>) could be attributed to the availability of free hydroxyl groups on the polymer side chain, as out of 24, only 9 conjugation sites were occupied by DOX.

The sizes of micelles either obtained via dialysis (during the final purification step) or by reconstituted PJJ-DOX in water were determined by DLS and TEM. As shown in Figure 2C, a bimodal size distribution was observed for both micelles attributed to the random attachment of DOX molecules, which in turn modulates the overall hydrophobic-to-hydrophilic ratio of the block copolymer and consequently, size upon self-assembly. The TEM images however suggested an absence of individual micelles with sizes greater than 100 nm in the sample, but the aggregation of micelles was evident and more prominent in the reconstitution sample owing to the freeze-drying stresses and could be the probable reason for the broader peaks in DLS (Figure 2C). As per TEM image analysis (by ImageJ), the size distribution histogram suggested that the majority of individual micelles were in the range of 30–40 nm along with some larger aggregates representing the second peak of the DLS graph.

The size distribution by volume in DLS also suggested that the majority of micelles fall in 30–40 nm (hydrodynamic diameter) along with some larger aggregates. We preferred to present the size distribution by volume here to demonstrate the change in size upon redispersion in an aqueous medium where a larger ratio is occupied by less than 100 nm micelles. Size distribution by intensity in DLS could be misleading in the bimodal distribution curve, as the intensity curve shows that the particles with bigger sizes are dominant particles owing to the stronger reflection of light. Based on the size results, it was decided to use reconstituted micelles for further evaluations since there were no substantial differences in size distribution.

Zeta potential of the PJJ-DOX micelles was recorded in HEPES buffer (20 mM, pH=7.2) and a charge close to neutral was observed (Figure S11, Supporting Information). Close to neutral surface charge was expected from PJJ-DOX micelles owing to the PEG corona where the micelles are usually sterically stabilized instead of electrostatically.<sup>[3,5]</sup> The in vitro drug release was performed via dialysis method at pH 5.0 mimicking intracellular environment in the presence of two different concentrations of commonly used reducing agent dithiothreitol (DTT).<sup>[21]</sup> A sustained release pattern was observed for DOX from PJJ-DOX micelles and as expected, a higher percentage of the drug was released in the presence of elevated DTT concentration (Figure 2F). However, even after 9 days, we did not observe even 50% of drug release (~43% release), which



is contrary to the objective of using stimuli-sensitive linkers to achieve triggered and complete release in the presence of stimuli. The probable reason for this could be associated with the micelle's core-corona structure, where the highly hydrophobic core contains all the DOX linked to PJI via the disulfide linker. DTT, being a hydrophilic substance could have limited access to the core and thus, in turn, cleaved fewer di-sulfide linkages. Slow drug release pattern has often been observed from micelles when the drug is being conjugated to the hydrophobic polymer<sup>[22]</sup> compared to hydrophilic polymer<sup>[21,23]</sup> via disulfide linking.

### 2.3. Evaluation of mPEG-b-PJI-OH and PJI-DOX on Cancer Cells

Cytotoxicity is an important parameter, which needs to be established for polymers that are intended to be used as drug delivery carriers. Therefore, we evaluated the toxicity profile of mPEG-b-PJI-OH on MDA-MB-231 cells. More than 90% of cells were found to be viable after 48 h of incubation for polymer concentrations up to 2 mg mL<sup>-1</sup> (Figure 3A). This result suggested the good tolerability of the polymer itself and minimum to no interference in the experiments aimed to determine the ability of PJI-DOX towards killing cancer cells.

DOX is a powerful anticancer drug, but also responsible for eliciting severe side effects, with cardiotoxicity being the most prominent one. Thus, selective release of DOX only within cancer cells is of prime importance in chemotherapy to avoid severe side effects. Prodrug formation of DOX by attaching it with polymer is a widely utilized approach to achieve this objective.<sup>[24]</sup> However, the most widely used synthetic polymers such as PEG and poly(N-(2-hydroxypropyl)methacrylamide) (HPMA) used for that purpose lacks biodegradability and has limited conjugation sites (for PEG). Moreover, unlike hydrophilic PEG or HPMA, mPEG-b-PJI being an amphiphilic polymer, demonstrated its ability to assemble into a core-corona structure as

reported above and could thus possibly protect the degradation of loaded cargo.<sup>[25]</sup> We earlier demonstrated this phenomenon by loading curcumin in a hydrophobic PDL core with the objective of increasing its stability.<sup>[3]</sup>

To establish the selective drug release capability of PJI-DOX in the presence of GSH, free DOX and PJI-DOX with equivalent concentrations of DOX (between 10–50 µg mL<sup>-1</sup>) were incubated with MDA-MB-231 cells with and without media containing GSH (10mM). As expected, being a highly toxic drug, DOX inhibited the growth of ≈75% cells at 50 µg mL<sup>-1</sup> concentration after 48 h incubation. No significant change in the toxicity pattern was observed for DOX in the presence of GSH. In contrast, PJI-DOX were found to be less toxic at similar DOX concentrations, where only ≈35% cell growth inhibition was observed after 48 h incubation. However, when PJI-DOX was incubated with cells in media containing GSH, a significant difference in toxicity was observed compared to without GSH treatment group (Figure 3A). This difference in cytotoxicity demonstrated by PJI-DOX can be attributed to the accelerated release of DOX due to the cleavage of disulfide linkage facilitated by GSH. Yet, PJI-DOX was not equally toxic as DOX on cancer cells, which can be ascribed to the limited disulfide cleavage and sustained release property exhibited by PJI-DOX micelles. As evident by the in vitro drug release evaluation, only ≈33% of drug release was observed after 48 h in the presence of 1 mM DTT (Figure 2F).

Further, to examine the cellular uptake efficiency of PJI-DOX micelles, confocal laser scanning microscopy (CLSM) was performed using DOX as an inherent fluorescent probe. The control samples did not produce any fluorescence as evident by CLSM images and thus not interfered in the analysis (Figure S12, Supporting Information). The fluorescence intensity of DOX was greatly reduced after conjugation with polymer followed by assembly into micelles, as evident by the fluorescence measurement of DOX and PJI-DOX in an aqueous medium (Figure S10B, Supporting Information). The quenching in fluorescence intensity of DOX after self-assembly into nanoparticles

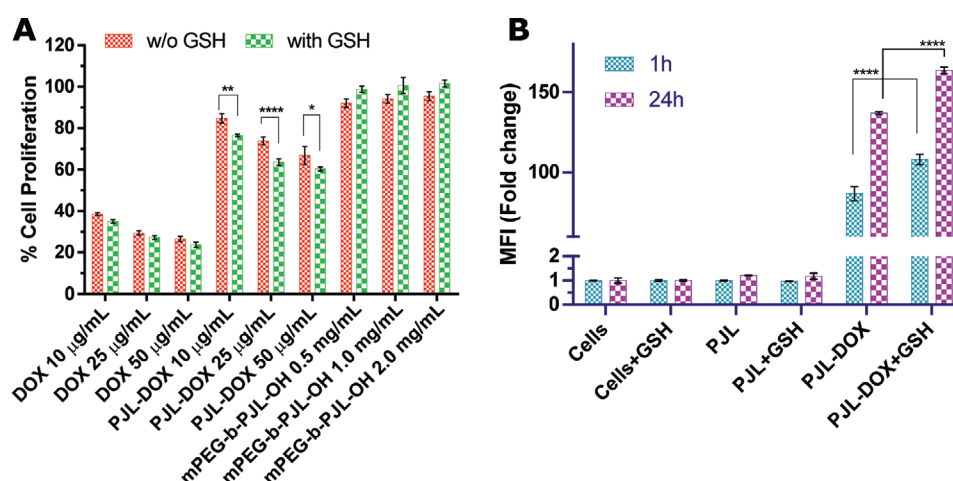


**Figure 3.** A) Inhibition of cell proliferation as detected by AlamarBlue assay after 48 h incubation of samples with MDA-MB-231 cells. The concentration of PJI-DOX was equivalent to the free DOX ( $n = 3$ ). B) Change in mean fluorescence intensity of PJI-DOX determined by flow cytometry after 1 and 24 h of incubation with cells. Experiments are done in media with and without 10 mM GSH to realize the cleavage of the disulfide bond. Statistical significance has been represented as extremely significant ( $****p < 0.0001$ ), extremely significant ( $***p = 0.0001-0.001$ ), very significant ( $**p = 0.001-0.01$ ), significant ( $*p = 0.01-0.05$ ).

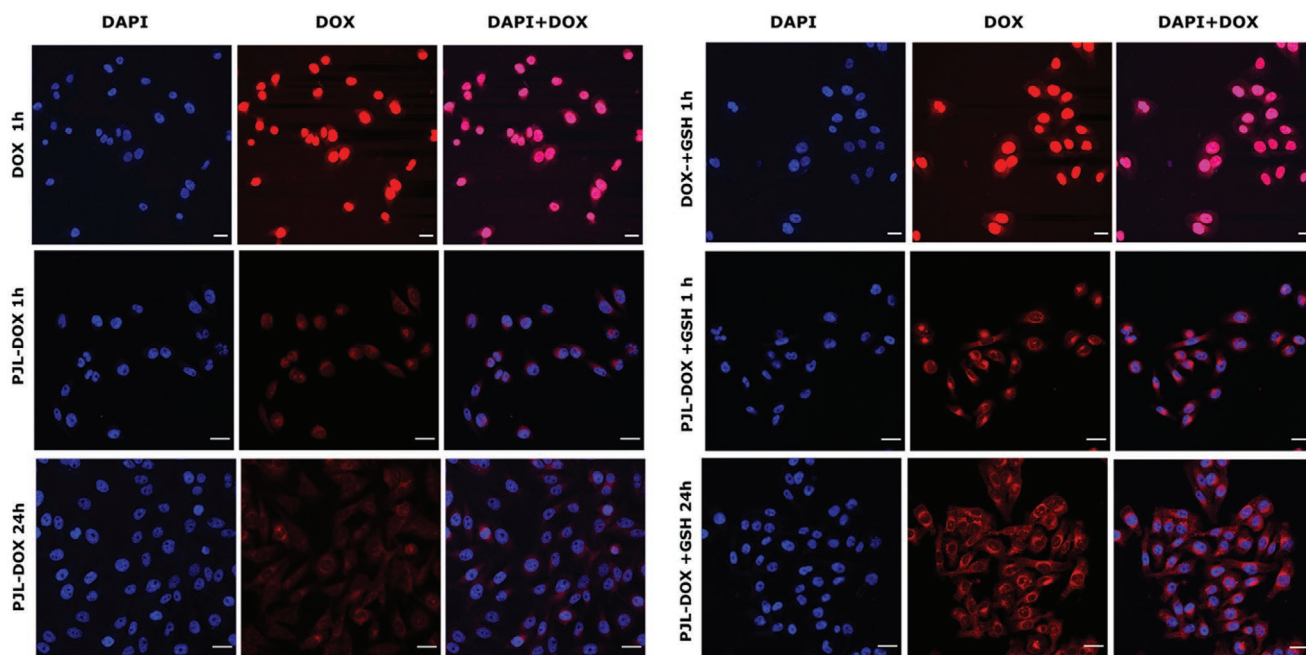


**Figure 4.** CLSM images of DOX and PJJ-DOX internalized in MDA-MB-231 cells after 1 h or 24 h incubation with or without GSH (10 mM). Cells were treated with  $5 \mu\text{g mL}^{-1}$  equivalent concentration of DOX. Scale bar corresponds to  $30 \mu\text{m}$ . Cell nucleus was stained with DAPI (blue), while DOX inherent red fluorescence was used to detect PJJ-DOX.

has been also reported recently.<sup>[26]</sup> We observed that free DOX abruptly enter into the nucleus to produce lethal effects owing to its mechanism of action, that is, inhibition of topoisomerase II enzyme found in the nucleus. On the other hand, the fluorescence observed from PJJ-DOX suggested that it is mostly surrounded by the nucleus instead of entering directly into the nucleus after 1 h of incubation. This observation again confirmed the absence of free DOX in conjugates and advised that DOX will slowly release from PJJ-DOX and enter the nucleus to exert the therapeutic action, as demonstrated in previous studies.<sup>[27]</sup>

To ascertain this phenomenon, CLSM images at 24 h time point were taken for PJJ-DOX and an increase in fluorescence intensity and DOX localization into the nucleus was observed. Moreover, a higher fluorescence intensity was observed for the sample containing GSH at similar time points in CLSM images (Figure 4). This increment in fluorescence intensity of DOX from PJJ-DOX can be attributed to the DOX release from micelles post cleavage of disulfide bond. To reconfirm the increment in fluorescence intensity, flow cytometry was performed and as shown in Figure 3B and Figure S13, Supporting Information, an increase in fluorescent intensity was clearly observed as the incubation time increases and in the presence of GSH in media. These observations demonstrate an intelligible advantage of delivering highly toxic drugs via conjugation approach (using stimuli sensitive linker) to avoid off-target toxicities.

### 3. Conclusion

In this study, we have, for the very first time, reported the synthesis and post-polymerization functionalization of novel

polymer PJJ, derived from renewable monomer jasmine lactone. We demonstrated that the combination of ROP and thiol-ene click reaction are capable of generating PJJ polymers with different pendant functional groups, which could be tuned as per the desired application. As a proof-of-concept, we have successfully demonstrated that PJJ polymer could be successfully utilized to deliver highly toxic drugs in a precise manner with an additional possibility of high drug loading. Interestingly, due to the amorphous nature of the polymer, we have not encountered any issue related to steric hindrance, which might considerably affect the reactivity of PJJ. We believe that this PJJ polymer with its excellent tunable property could bring on a paradigm shift in the functional materials category. Our future studies will thus be focused on developing PJJ polymer with multi-functional reactive groups in a single chain with the possibility to prepare dual stimuli-sensitive drug delivery systems. We postulate that the combination of endogenous with exogenous stimuli in designing smart drug delivery systems would certainly bring more control on precise drug release at target sites in sufficient amounts and in the long run, probably solve the issue of incomplete drug release.

### 4. Experimental Section

Experimental details are provided in the Supporting Information.

### Supporting Information

Supporting Information is available from the Wiley Online Library or from the author.



## Acknowledgements

This work was supported by the Academy of Finland (projects #309794, 309374) (K.K.B. and J.M.R.). Swedish Cultural Foundation is acknowledged for financial support (E.Ö.). The authors would also like to thank Mr. Mitesh Modi, Sterling Biotech Ltd., India, for providing a gift sample of the drug (DOX). Electron microscopy imaging was performed in the Electron Microscopy Laboratory, Institute of Biomedicine, University of Turku, and confocal microscopy imaging and flow cytometry was performed at the Cell Imaging and Cytometry Core, Turku Bioscience Centre, Turku, Finland, with the support of Biocenter Finland. K.K.B. would like to thank Prof. Cameron Alexander, The University of Nottingham, U.K. for his guidance and support.

## Conflict of Interest

The authors declare no conflict of interest.

## Data Availability Statement

The data that support the findings of this study are available from the corresponding author upon reasonable request.

## Keywords

block copolymer micelles, functional polymers, poly(jasmine lactone), polymer-drug conjugate, redox responsive drug delivery, renewable polyesters, ring-opening polymerization

Received: February 26, 2021

Revised: May 13, 2021

Published online: June 14, 2021

- [1] K. K. Bansal, J. M. Rosenholm, *Ther. Delivery* **2020**, *11*, 297.
- [2] G. Trubitsyn, V. N. Nguyen, C. Di Tommaso, G. Borchard, R. Gurny, M. Möller, *Eur. J. Pharm. Biopharm.* **2019**, *142*, 480.
- [3] K. K. Bansal, J. Gupta, A. Rosling, J. M. Rosenholm, *Saudi Pharm. J.* **2018**, *26*, 358.
- [4] K. K. Bansal, D. Kakde, L. Purdie, D. J. Irvine, S. M. Howdle, G. Mantovani, C. Alexander, *Polym. Chem.* **2015**, *6*, 7196.
- [5] K. K. Bansal, E. Özliseli, G. K. Saraogi, J. M. Rosenholm, *Pharmaceutics* **2020**, *12*, 726.
- [6] a) D. Kakde, V. Taresco, K. K. Bansal, E. P. Magennis, S. M. Howdle, G. Mantovani, D. J. Irvine, C. Alexander, *J. Mater. Chem. B* **2016**, *4*, 7119; b) J. Wik, K. K. Bansal, T. Assmuth, A. Rosling, J. M. Rosenholm, *Drug Delivery Transl. Res.* **2020**, *10*, 1228.
- [7] X. Xu, P. E. Saw, W. Tao, Y. Li, X. Ji, S. Bhasin, Y. Liu, D. Ayyash, J. Rasmussen, M. Huo, J. Shi, O. C. Farokhzad, *Adv. Mater.* **2017**, *29*, 1700141.
- [8] a) I. Ekladious, Y. L. Colson, M. W. Grinstaff, *Nat. Rev. Drug Discovery* **2019**, *18*, 273; b) P. Thakor, V. Bhavana, R. Sharma, S. Srivastava, S. B. Singh, N. K. Mehra, *Drug Discovery Today* **2020**.
- [9] A. Xie, S. Hanif, J. Ouyang, Z. Tang, N. Kong, N. Y. Kim, B. Q. D. Patel, B. Shi, W. Tao, *EBioMedicine* **2020**, *56*, 102821.
- [10] G. Becker, F. R. Wurm, *Chem. Soc. Rev.* **2018**, *47*, 7739.
- [11] R. Bhatt, P. de Vries, J. Tulinsky, G. Bellamy, B. Baker, J. W. Singer, P. Klein, *J. Med. Chem.* **2003**, *46*, 190.
- [12] a) R. Duncan, *J. Controlled Release* **2014**, *190*, 371; b) R. Duncan, *J. Drug Targeting* **2017**, *25*, 759.
- [13] X. Tang, M. Hong, L. Falivene, L. Caporaso, L. Cavallo, E. Y. X. Chen, *J. Am. Chem. Soc.* **2016**, *138*, 14326.
- [14] a) W. Chen, L. A. Shah, L. Yuan, M. Siddiq, J. Hu, D. Yang, *RSC Adv.* **2015**, *5*, 7559; b) Z. Deng, S. Liu, *J. Controlled Release* **2020**, *326*, 276; c) S. Mollazadeh, M. Mackiewicz, M. Yazdimaghani, *Mater. Sci. Eng., C* **2021**, *118*, 111536; d) Y. Su, Y. Hu, Y. Du, X. Huang, J. He, J. You, H. Yuan, F. Hu, *Mol. Pharmaceutics* **2015**, *12*, 1193.
- [15] X. Ma, E. Özliseli, Y. Zhang, G. Pan, D. Wang, H. Zhang, *Biomater. Sci.* **2019**, *7*, 634.
- [16] M. T. Martello, A. Burns, M. Hillmyer, *ACS Macro Lett.* **2012**, *1*, 131.
- [17] A. B. Lowe, *Polym. Chem.* **2014**, *5*, 4820.
- [18] A. J. D. Magenau, J. W. Chan, C. E. Hoyle, R. F. Storey, *Polym. Chem.* **2010**, *1*, 831.
- [19] A. D. Hanna, A. Lam, S. Tham, A. F. Dulhunty, N. A. Beard, *Mol. Pharmacol.* **2014**, *86*, 438.
- [20] a) Y. Shi, H. Zhu, Y. Ren, K. Li, B. Tian, J. Han, D. Feng, *Colloid Polym. Sci.* **2017**, *295*, 259; b) T. Sim, J. E. Kim, N. H. Hoang, J. K. Kang, C. Lim, D. S. Kim, E. S. Lee, Y. S. Youn, H.-G. Choi, H.-K. Han, K.-Y. Weon, K. T. Oh, *Drug Delivery* **2018**, *25*, 1362.
- [21] D. Zhao, H. Zhang, S. Yang, W. He, Y. Luan, *Int. J. Pharm.* **2016**, *515*, 281.
- [22] a) P. Zhang, H. Zhang, W. He, D. Zhao, A. Song, Y. Luan, *Biomacromolecules* **2016**, *17*, 1621; b) Y. Guo, P. Zhang, Q. Zhao, K. Wang, Y. Luan, *Macromol. Biosci.* **2016**, *16*, 420; c) Q. Zhang, J. He, M. Zhang, P. Ni, *J. Mater. Chem. B* **2015**, *3*, 4922.
- [23] D. Zhao, J. Wu, C. Li, H. Zhang, Z. Li, Y. Luan, *Colloids Surf., B* **2017**, *155*, 51.
- [24] V. Hanušová, I. Boušová, L. Skálová, *Drug Metab. Rev.* **2011**, *43*, 540.
- [25] a) K. Miyata, R. J. Christie, K. Kataoka, *React. Funct. Polym.* **2011**, *71*, 227; b) G. Yu, Q. Ning, Z. Mo, S. Tang, *Artif. Cells, Nanomed., Biotechnol.* **2019**, *47*, 1476; c) K. Bansal, N. Lariya, *Chron. Pharm. Sci.* **2018**, *2*, 534.
- [26] Y. Wang, X. Wang, F. Deng, N. Zheng, Y. Liang, H. Zhang, B. He, W. Dai, X. Wang, Q. Zhang, *J. Controlled Release* **2018**, *279*, 136.
- [27] a) X. Su, B. Ma, J. Hu, T. Yu, W. Zhuang, L. Yang, G. Li, Y. Wang, *Bioconjugate Chem.* **2018**, *29*, 4050; b) Y. Liang, S. Li, X. Wang, Y. Zhang, Y. Sun, Y. Wang, X. Wang, B. He, W. Dai, H. Zhang, X. Wang, Q. Zhang, *J. Controlled Release* **2018**, *275*, 129; c) S. Cai, A. A. B. Alhowyan, Q. Yang, W. C. M. Forrest, Y. Shnyder, M. L. Forrest, *J. Drug Targeting* **2014**, *22*, 648.